Chemical Science

ROYAL SOCIETY OF CHEMISTRY

EDGE ARTICLE

View Article Online
View Journal | View Issue

Cite this: *Chem. Sci.*, 2021, **12**, 3702

All publication charges for this article have been paid for by the Royal Society of Chemistry

Received 7th October 2020
Accepted 18th January 2021

DOI: 10.1039/d0sc05550f

rsc.li/chemical-science

Photocatalyst-independent photoredox ring-opening polymerization of *O*-carboxyanhydrides: stereocontrol and mechanism†

Yongliang Zhong,[a] Quanyou Feng,[ab] Xiaoqian Wang,[a] Lei Yang,[b] Andrew G. Korovich,[c] Louis A. Madsen[c] and Rong Tong *[a]

Photoredox ring-opening polymerization of *O*-carboxyanhydrides allows for the synthesis of polyesters with precisely controlled molecular weights, molecular weight distributions, and tacticities. While powerful, obviating the use of precious metal-based photocatalysts would be attractive from the perspective of simplifying the protocol. Herein, we report the Co and Zn catalysts that are activated by external light to mediate efficient ring-opening polymerization of *O*-carboxyanhydrides, without the use of exogenous precious metal-based photocatalysts. Our methods allow for the synthesis of isotactic polyesters with high molecular weights (>200 kDa) and narrow molecular weight distributions (M_w/M_n < 1.1). Mechanistic studies indicate that light activates the oxidative status of a Co^{III} intermediate that is generated from the regioselective ring-opening of the *O*-carboxyanhydride. We also demonstrate that the use of Zn or Hf complexes together with Co can allow for stereoselective photoredox ring-opening polymerizations of multiple racemic *O*-carboxyanhydrides to synthesize syndiotactic and stereoblock copolymers, which vary widely in their glass transition temperatures.

Introduction

Polyesters have long been considered as environmentally friendly alternatives to petrochemical-based polyolefins because of their degradability and biocompatibility.[1–5] Among many degradable polyesters, poly(α-hydroxy acids) (PAHAs) have been regarded as a type of industry applicable, degradable, and biocompatible polyester, and a few of them (*e.g.*, poly(lactic-*co*-glycolic acid)) have been approved by the FDA (U.S. Food and Drug Administration) for clinical applications. However, the utility of PAHAs for applications that demand physico-mechanical and thermal properties, such as high stiffness and high glass transition temperatures (T_gs), is greatly limited by the lack of side-chain functionality in PAHAs and in their lactone monomers.[6–8] Early work by the Baker group shows that PAHAs synthesized from functionalized lactides (LAs) present a wide range of T_gs from −46 °C to 100 °C.[9–11] Unfortunately, the multi-step synthesis of functionalized LAs is challenging; monomers are afforded in low yields; while the polymerization reactivity significantly drops upon the introduction of pendant groups (Scheme 1, route i).[9,12,13]

Alternative strategies have been developed to access monomers that can be easily synthesized and polymerized. Noticeably, a five-membered heterocycle 1,3-dioxolan-4-one that bears both ester and acetal groups has been recently developed by Miller[14] and Shaver groups (Scheme 1, route ii).[15,16] Either through copolymerization with LAs for acetal retention,[14] or ring-opening polymerizations (ROPs) *via* the deliberation of formaldehyde, this monomer provides an inexpensive strategy to prepare PAHAs. However, the ROP strategy for 1,3-dioxolan-4-one requires further development as the obtained polymers had

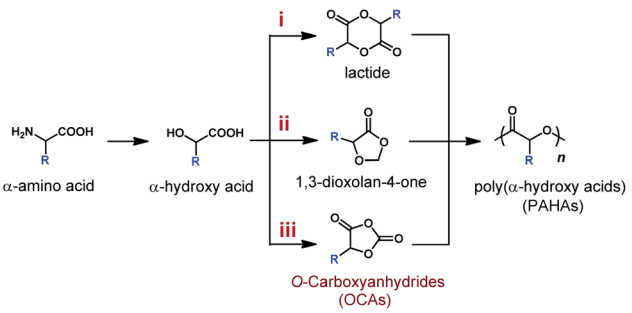

Scheme 1 Synthetic routes of poly(α-hydroxy acids) (PAHAs) from α-amino acids and α-hydroxy acids *via* different monomers.

[a]*Department of Chemical Engineering, Virginia Polytechnic Institute and State University, 635 Prices Fork Road, Blacksburg, Virginia, 24061, USA. E-mail: rtong@vt.edu*

[b]*Key Laboratory for Organic Electronics and Information Displays, Jiangsu Key Laboratory for Biosensors, Institute of Advanced Materials, Jiangsu National Synergetic Innovation Center for Advanced Materials, Nanjing University of Posts and Telecommunications, 9 Wenyuan Road, Nanjing, 210023, China*

[c]*Department of Chemistry, Virginia Polytechnic Institute and State University, 1040 Drillfield Drive, Blacksburg, Virginia, 24061, USA*

† Electronic supplementary information (ESI) available. See DOI: 10.1039/d0sc05550f

relatively low molecular weights (MWs, <20 kDa) due to side reactions, and the ROP procedures demand constant removing of formaldehyde from the reaction solution.[15,16]

Since 2006, *O*-carboxyanhydrides (OCAs) have emerged as an alternative class of highly active monomers with pendant functional groups for the synthesis of functionalized PAHAs (Scheme 1, route iii).[6,17,18] OCAs are readily prepared from amino acids or hydroxyl acids; however, the current ROP methods using organocatalysts cannot synthesize stereoregular and high-MW polyesters (Scheme 2A), and they cannot mediate stereoselective ROP of OCAs to prepare functionalized polyesters with different tacticities.[19–23] Note that tacticity is one of the most critical determinants of the physical and mechanical properties of a polymer.[24,25] For example, the stereocontrolled ROP of *rac*- and *meso*-lactide can result in a wide range of poly(lactide) microstructures with different T_gs.[24] On the other hand, many well-defined metal catalysts (*e.g.*, Zn and Hf complexes) that mediate stereoselective living and polymerization of lactones have been evaluated for stereoselective ROP of OCAs (Scheme 2B).[24,26–30] Nevertheless, extensive utilization of metal-catalyzed ROP of OCAs was limited because of their complicated reactivity and inability to prepare high-MW polyesters.[21,22] We have recently reported the controlled stereoselective ROPs of OCAs by using Ni/Zn/Ir-mediated photoredox ROP method,[22,31] and Co/Zn-mediated electrochemical ROP (eROP) of OCAs[32] that all provide high MW (over 140 kDa) functionalized polyesters with narrow MW distributions ($Đ$ < 1.1). Importantly, both photoredox ROP and eROP allow for tuning the polymerization kinetics by turning the light or electricity on or off.[31,32]

Despite the high efficiency, the photoredox ROP protocol requires expensive precious metal photocatalysts for decarboxylation, and only isoselective polymerization was achieved.[22,31] Precious metal-based photocatalysts, such as Ru and Ir complexes, impose significant environmental footprints due to terrestrial scarcity.[33,34] The utilization of earth-abundant metals as visible-light photocatalysts has recently gained great interest in order to develop sustainable photocatalysts.[35] Recently reported light-induced metal catalysts include Cu,[36–39] Co,[40–43] Ni,[34,44–46] Mn,[47–49] Ce[50–53] and Fe[54,55] complexes. Such metal complexes usually involve photoinduced single-electron transfer between the substrate and the catalyst, and allow for reactions that occur directly from their photoexcited states, without the assistance of exogenous photocatalysts that harvest light to transfer electron or energy.[56,57] However, the use of earth-abundant photocatalysts in photo-polymerization could be hampered by the short excited-state lifetime, which is usually picoseconds to nanoseconds for first-row transition metals.[58,59] In our initial report on the use of Co/Zn-mediated eROP of OCAs, we found that Co complexes could replace Ni/Ir in the photoredox ROP.[32] To our knowledge, the use of photoactive organometallic complexes as polymerization catalysts has been rarely achieved.[60] Considering our eROP method usually involves laborious workup to separate electrolytes from the solvent after electrochemical reactions,[32] it is therefore crucial to develop viable earth-abundant metal catalysts that can mediate controlled polymerization to prepare high-MW polyesters with different tacticities.

Herein, we report the development of photoactive Co catalysts that are amenable to efficiently polymerize enantiopure

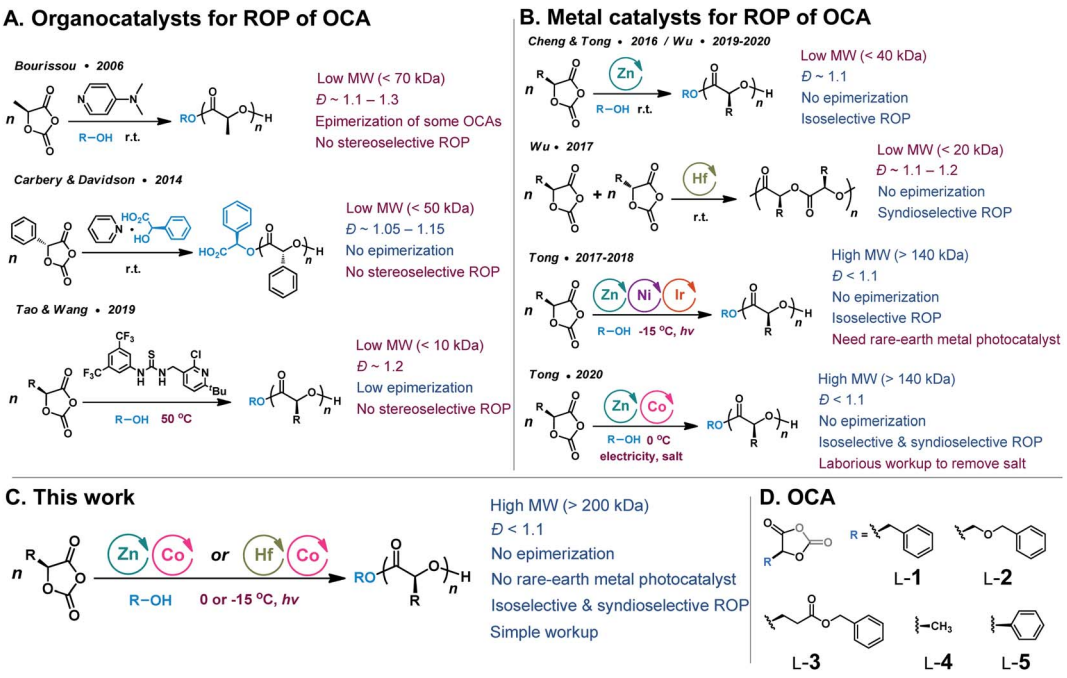

Scheme 2 Ring-opening polymerization (ROP) methods of *O*-carboxyanhydrides (OCAs) for accessing functionalized polyesters: (A) the use of organocatalysts; (B) the use of metal catalysts; (C) Co/Zn or Co/Hf-mediated stereoselective photoredox ROPs in this work; (D) chemical structures of OCAs used in this work. MW, molecular weight. Colors in (A–C) highlight pros (blue) and cons (red) of different synthetic methods.

OCAs in the presence of Zn or Hf complexes, resulting in isotactic polymers with unprecedented high MWs (>200 kDa) and narrow MW distributions ($Đ$ < 1.1, Scheme 2C). Mechanistic studies implicate our Co complexes as underexplored alternatives to precious metal photocatalysts. We also demonstrate that these metal complexes can be used to prepare various syndiotactic and stereoblock polyesters from different racemic OCA monomers, with T_g values ranging over ~100 °C (Scheme 2C and D).

Results and discussion

Discovery and optimization of Co/Zn complexes for photoredox ring-opening polymerization

In our prior studies on Co/Zn-mediated eROP,[32] we found that Co^{II} complexes could replace both the Ni catalyst and the Ir photocatalyst, and mediated photoredox ROP of OCA at 0 °C when irradiated with light from a blue LED (300–500 nm). Several Co^{II} complexes could lead to controlled photoredox ROP with M_n values close to MW_{cal} of 103.7 kDa at the [L-**1**]/[**Zn-1**] ratio of 700/1 (Fig. S1;† L-**1**, phenyl *O*-carboxyanhydride, see Scheme 2D; M_n, number-average MW; MW_{cal}, calculated MW based on feeding ratios). However, when the [L-**1**]/[**Zn-1**] ratio was elevated to 800/1, only 3 Co^{II} complexes led to controlled photoredox ROP with M_n values close to MW_{cal} of 118.5 kDa at 0 °C (Fig. S1†). Specifically, **Co-1** (**Co-1** = (bpy)Co[$N(SiMe_3)_2$]$_2$, bpy = 2,2′-bipyridine), **Zn-1** (**Zn-1** = Zn[$N(SiMe_3)_2$]$_2$), and BnOH are all necessary for this controlled photoredox ROP (Table S1†). However, when the initial [L-**1**]/[**Co-1**]/[**Zn-1**] ratio was 900/1/1, monomer conversion was only 43.7% (Fig. 1A, green line), indicating the occurrence of side reactions. When the photoredox reaction temperature was decreased to −15 °C (Scheme 3), the M_n values of the poly(L-**1**) products increased linearly with initial [L-**1**]/[**Co-1**]/[Zn] ratio up to 1100/1/1 and were slightly higher than the MW_{cal} values (Fig. 1A, blue line). Note that at this temperature, the $Đ$ values of all of the obtained polymers were <1.1 (Fig. 1A; gel-permeation chromatography traces in Fig. S2†). Additionally, the MWs of poly(L-**1**) showed linear correlation with the conversion of L-**1** at the initial [L-**1**]/[**Co-1**]/[**Zn-1**] ratio of 1000/1/1 (Fig. S3†). No epimerization of the α-methine hydrogen was observed in the homodecoupled ^{1}H NMR spectra of the polymers, including high-MW poly(L-**1**) (M_n = 215.2 kDa, Fig. S4†), suggesting that the Co complex did not affect the chirality of L-**1** during the ROP. Moreover, electrospray ionization mass spectrometry (ESI-MS) analysis of oligo(L-**1**) confirmed attachment of the BnO – group to the oligomer (Fig. S5†), indicating that a Zn–alkoxide was involved in ring-opening and chain propagation. Note that nearly all metal complexes can be readily removed by simply washing the polymer with methanol, as indicated by inductively coupled plasma mass spectrometry (Table S2†).

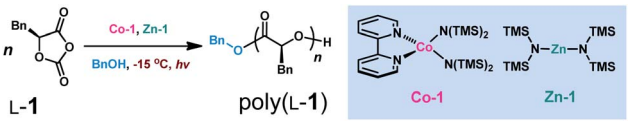

Scheme 3 Photoredox controlled ring-opening polymerization of L-**1** mediated by **Co-1**/**Zn-1**.

We then examined the kinetics of photoredox ROP of L-**1** at −15 °C by varying the concentration of each reaction component. The reaction was first-order with respect to L-**1** (Fig. 1B). To explore whether Co and Zn catalysts formed a coordinate complex to mediate the polymerization, we fixed the Co/Zn ratio at 1/1 in the kinetic study and found the reaction order was 5.06 ± 0.21 (Fig. S5†); whereas the reaction orders with respect to **Co-1**, **Zn-1** and BnOH were 2.33 ± 0.20, 2.64 ± 0.03, and 0 respectively (Fig. S6†). These results indicate that no formation of Co–Zn complex during the photoredox ROP, and the rate of chain propagation was independent of BnOH concentration. Therefore the kinetics of the photoredox ROP of L-**1** follows an overall kinetic law of the form:

$$-\mathrm{d}[\text{L-}\mathbf{1}]/\mathrm{d}t = k_p[\mathbf{Co\text{-}1}]^{2.33}[\mathbf{Zn\text{-}1}]^{2.64}[\text{L-}\mathbf{1}]^{1} \quad (1)$$

where k_p is the rate constant of chain propagation. These observed kinetic rates are different from those in eROP even using the same Co/Zn catalysts (Fig. S7†), presumably because of different reaction temperatures (eROP at 0 °C).

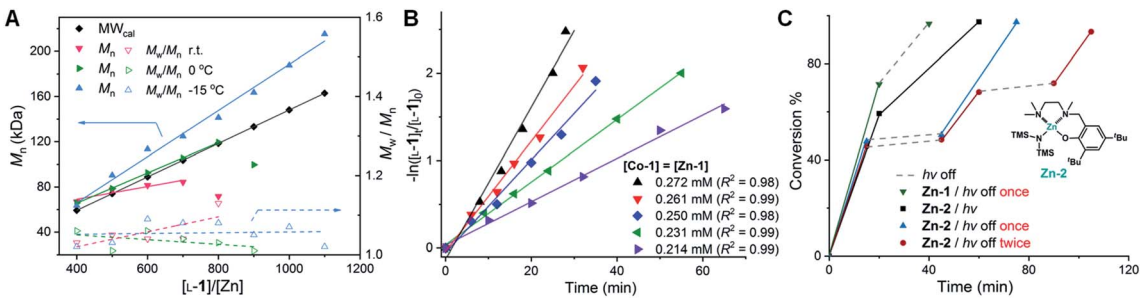

Fig. 1 Photoredox controlled ring-opening polymerization of L-**1** mediated by Co/Zn complexes. (A) Plots of M_n and molecular weight distribution (M_w/M_n) of poly(L-**1**) *versus* [L-**1**]/[**Zn-1**] at various reaction temperatures ([**Co-1**]/[**Zn-1**]/[BnOH] = 1/1/1); MW_{cal}, molecular weight calculated from monomer/catalyst ratio; M_n, number-average molecular weight; M_w, weight-average molecular weight. * and ** indicated incomplete monomer conversions. (B) Logarithmic plots of L-**1** conversion *versus* time at various **Zn-1** concentrations, showing first-order kinetics. [L-**1**] = 150 mM; [**Co-1**]/[**Zn-1**]/[BnOH] = 1/1/1; reaction temperature, −15 °C. (C) Dependence of the rate of L-**1** conversion on the presence or absence of light irradiation onto the reaction at −15 °C ([L-**1**]/[**Co-1**]/[**Zn-2**]/[BnOH] = 800/1/1/1; [L-**1**] = 208.4 mM). The dashed lines indicate periods during which no light was applied; while solid lines indicate the period during which light was applied.

We then examined whether Co/Zn-mediated photoredox ROP could allow for the temporal modulation of polymerization rates by turning the light on or off. Similar to our previous studies using Ni/Zn/Ir catalysts,[31] we found that in the presence of **Zn-2** (Fig. 1C), a Zn complex with a tridentate ligand, irradiation of the reaction solution for 15 min resulted in 47% conversion of L-**1** ([L-**1**]/[**Co-1**]/[**Zn-2**]/[BnOH] = 800/1/1/1). When the light was then turned off, the conversion of L-**1** slightly increased to 50% over 30 min. Once the current was resumed, the polymerization revived with a conversion of L-**1** to 97% over 30 min (Fig. 1C, blue line). In contrast, in a similar reaction mediated by **Zn-1**, consumption of L-**1** continued even after the light was turned off (Fig. 1C, green line). Such "light on–off" ROP could be repeated twice: each time the light was turned off, the ROP almost stopped, and it proceeded again rapidly when the irradiation was resumed (Fig. 1C, red line).

With a set of optimized conditions in hand, we explored the generality of the Co/Zn-mediated photoredox polymerization by carrying out reactions of other OCAs (L-**2**, L-**3**, L-**4**, and L-**5**, and their structures in Scheme 2D; Table S3†). In all instances, polymerization proceeded smoothly, as was the case for the formation of poly(L-**1**); the M_n values of the obtained polymers were close to the MW_{cal} values, most of $Đ$ values were <1.1, and the α-methine hydrogens did not epimerize (Fig. S8–S11†). Note that considerable epimerization of L-**5**, which has an acidic α-methine proton, is often observed during ROP,[20,21,61] but this was not the case in our system (Fig. S11†). Moreover, diblock copolymers and a triblock copolymer could be readily prepared by sequential addition of the monomers, and excellent control of the M_n and $Đ$ values was achieved (Table S4 and Fig. S13–S21†).

Electrochemistry and photophysics studies of Co complex in photoredox ring-opening polymerization

Photoredox catalysts such as Ir- or Ru-based polypyridyl complexes are often used in the presence of an exogenous reductant or oxidant.[33,62–64] Unlike in nearly all photopolymerizations that use one photocatalyst to affect redox chemistry and a different catalyst to re-generate free radicals or radical ions for chain propagation,[65–70] in our method a single **Co-1** complex is responsible both for ring-opening of the OCAs and for photoredox decarboxylation to accelerate chain propagation. Given that no obvious oxidant or reductant was present in the reaction mixture and that light was required, we carried out electrochemistry and photophysics experiments to probe the mode of action of the Co catalyst.

The cyclic voltammogram of **Co-1** exhibited a reversible redox wave with an $E^{red}_{1/2}[Co^{III}/Co^{II}]$ of 0.746 V *versus* SCE (SCE, saturated calomel electrode, the value equals 0.366 V *vs.* Fc^+/Fc; Fc, ferrocene; Fig. 2A). Notably, the addition of **Ir-1** ($E^{red}_{1/2}[*Ir^{III}/Ir^{II}]$ = 1.21 V *versus* SCE)[71] resulted in incomplete monomer conversion (Scheme 4; Table S5,† entry 2), presumably because electron transfer between **Co-1** and **Ir-1** led to inefficient chain propagation. This was also observed when adding another highly oxidizing photocatalyst, $Ru(bpz)_3^{2+}$ (bpz = 2,2′-bipyrazyl; $E^{red}_{1/2}[*Ru^{III}/Ru^{II}]$ = 1.45 V *versus* SCE).[72] In contrast,

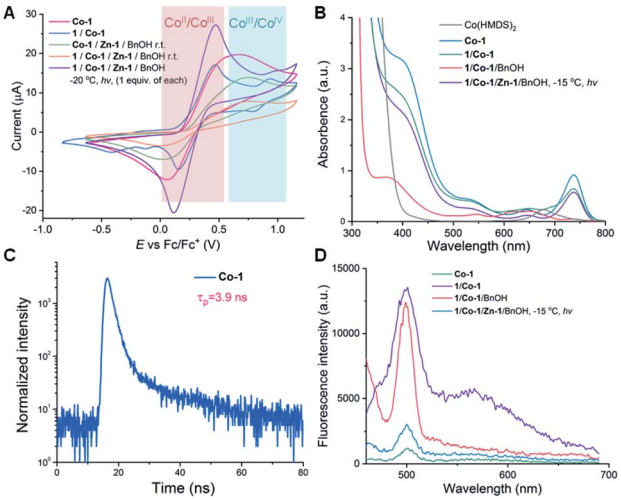

Fig. 2 Electrochemical and photophysical studies of the photoredox decarboxylation reactions mediated by **Co-1**. (A) Cyclic voltammograms of **Co-1** and the ring-opening reaction mixtures (1 equiv. of each) at various conditions. Scan rate: 100 mV s^{-1}. Solvent: 0.1 M tetrabutylammonium hexafluorophosphate in THF. Initial scanning direction: zero to positive. (B) UV/vis absorption spectra of **Co-1** and the reaction mixtures (1 equiv. of each). [Co] = 2.0 mM in THF in all samples. (C) Photoluminescence decay of **Co-1** recorded in deaerated THF with excitation at 350 nm. (D) Emission spectra of **Co-1** and the reaction mixtures (1 equiv. of each) with the excitation at 435 nm. [Co] = 2.0 mM in THF in all samples.

photocatalysts that have lower excited-state reduction potentials (*e.g.*, $Ru(bpy)_3^{2+}$ and *fac*-$Ir(ppy)_3$; ppy = 2-phenylpyridine)[62] than those of **Ir-1** did not affect the polymerization results

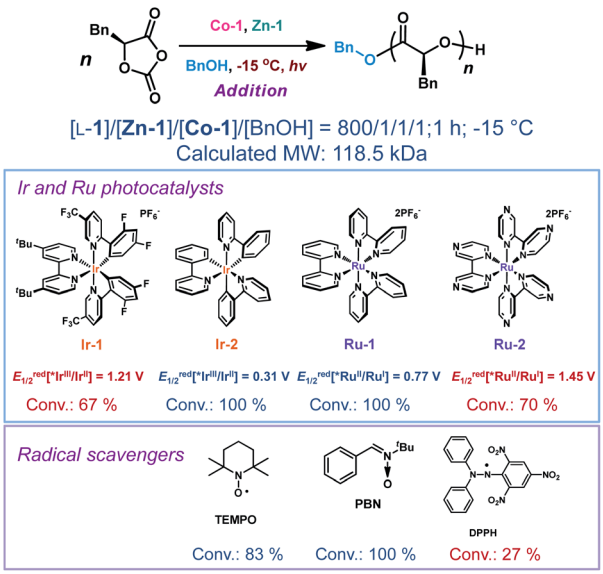

Scheme 4 Effects of the addition of precious-metal photocatalysts and radical scavengers into the photoredox ring-opening polymerization of L-**1**.[a] [a]Abbreviations: conv., monomer conversion; TEMPO, 2,2,6,6-tetramethylpiperidine-*N*-oxyl; PBN, *N*-*tert*-butyl-α-phenylnitrone; DPPH, 2,2-diphenyl-1-picrylhydrazyl. For all polymerization reactions, [**Co-1**] = [**Zn-1**] = [BnOH]. $E^{red}_{1/2}$ values for photocatalysts are based on ref. 62 Detailed polymerization data in Table S5.†

(entries 3–4). The results indicated that the use of highly oxidative photocatalysts (**Ir-1** and **Ru-2** in Scheme 4) could disturb the electron transfer process in the photoexcited Co^{III} intermediate and resulted in observed inefficient polymerization.

The involvement of radical intermediates in Co/Zn-mediated photoredox ROP was confirmed by the use of radical scavengers. We found that nitroxide-based radical scavengers, such as 2,2,6,6-tetramethylpiperidine-*N*-oxyl (TEMPO), and *N*-*tert*-butyl-α-phenylnitrone, were ineffective at inhibiting the polymerization (Scheme 4; Table S5,† entries 6 and 7), different from that in Ni/Ir-mediated photoredox reaction.[22] This may be due to TEMPO's inability to trap radicals in certain organometallic reactions.[73,74] However, another powerful radical scavenger, 2,2-diphenyl-1-picrylhydrazyl (DPPH), effectively disrupted chain propagation (entry 8), indicating the possible formation of the photoexcited radical species.

We then found that the absorption spectrum of **Co-1** exhibited a maximum around 398 nm that did not correspond to the ligand (bpy, Fig. 2B). Upon photoexcitation at 298 K, a photoluminescence band with a lifetime of 3.9 ns was observed (Fig. 2C), which is longer than many first-row transition metal complexes.[57,75] This band likely corresponds to a metal-to-ligand charge-transfer excited state,[76] a possibility that was supported by density functional theory calculations: the lowest unoccupied molecular orbital was located exclusively on the π-system of the bpy ligand in **Co-1**, whereas the highest occupied molecular orbital (HOMO), HOMO−1, HOMO−3 and HOMO−4, were dominated by contributions from the Co d_{yz}, d_{xz}, d_{xy}, and $d_{x^2-y^2}$ orbitals (Fig. S22†).

Additionally, L-**1**/**Co-1** exhibited a metal-to-ligand charge-transfer absorption band (Fig. 2B). Notably, the time-dependent density functional theory computed absorption spectra of both **Co-1** and L-**1**/**Co-1** are in good agreement with our experimental spectra (Fig. S23†). We also noticed that the intensity of the emission band at 499 nm was 11.6 times that of **Co-1**; and a broad peak with a maxima at 567 nm was also only found in L-**1**/**Co-1** (excitation wavelength, 435 nm; Fig. 2D). This suggested that a transient photoactive cobaltacycle adduct formed after oxidative insertion of **Co-1** into L-**1**. Attempts to isolate such photoactive Co^{III} species were unsuccessful. Because no Co^{II}/Co^{I} and minimal Co^{IV}/Co^{III} (1.308 V *versus* SCE) redox couples were observed in the mixture of **Co-1**, **Zn-1**, BnOH and L-**1** (1 equiv. of each) under irradiation with light at −20 °C (Fig. 2A), the photoexcited Co^{III} complex (**II** in Scheme 5) likely functioned as a viable photo-oxidant. Calculations based on the photophysical and electrochemical results indicated that such a Co^{III} intermediate had an estimated $E^{red}_{1/2}(*Co^{III}/Co^{II})$ of 2.878 V (Table S6†). Given the oxidation potential of the amino acid carboxylate ($E^{red}_{1/2}$ = 0.832 V *vs.* SCE for *N*-(carbobenzyloxy)-L-phenylalanine; Table S6†) and literature reports,[77,78] the photoexcited Co^{III}-mediated decarboxylation process was thermodynamically feasible.[77]

Next we explored the state of the Co complex after photoredox decarboxylation. Comparison of cyclic voltammograms (Fig. 2A), the absorption and fluorescence spectra (Fig. 2B and D), and magnetic moments of **Co-1** alone (4.78 μ_B) with those of

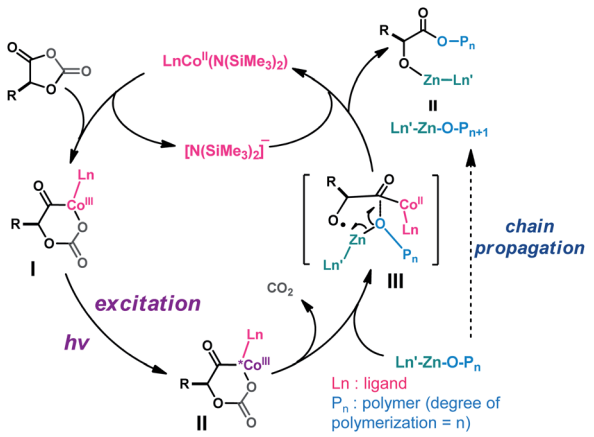

Scheme 5 Proposed Co/Zn-mediated photoredox ring-opening polymerization of *O*-carboxyanhydrides.

the L-**1**/**Co-1**/**Zn-1**/BnOH mixture (1 equiv. of each) irradiated at −15 °C (4.94 μ_B) indicates that a Co^{II} complex was likely to have been regenerated after the decarboxylation. Note that the magnetic moment of a L-**1**/**Co-1** mixture decreased substantially from 4.78 to 4.16 μ_B, owing in part to the formation of a Co^{III} adduct, which is assumed to have a lower magnetic moment than Co^{II}.[79] On this basis, we hypothesize that the reduced Co^{II} species and alkoxy radical **III** are likely generated *via* the successive loss of CO_2 (Scheme 5). We note that considering the low-intensity absorption of the L-**1**/**Co-1**/BnOH mixture (Fig. 2B), it is less likely that a photoexcited Co–alkoxide species was involved in the decarboxylation.

Regioselective Co/Zn-mediated ring-opening of OCAs

We then investigated whether Co^{II} could oxidatively add to the OCA in a regioselective manner (Scheme 6). We initially attempted to use ^{13}C NMR spectroscopy to study the reaction of L-**1** mediated by **Co-1**, **Zn-1**, and BnOH (1 equiv. of each), but the presence of the paramagnetic **Co-1** complex resulted in less informative NMR spectra. We found that the use of ^{13}C-labeled L-**1** allowed us to conveniently monitor the reaction intermediates in ^{13}C NMR, because broad peaks can be avoided when using ^{13}C-labeled compounds in ^{13}C NMR to decrease nuclear relaxation rates.[80] To differentiate the insertion site of Co^{II} complex in OCA, we prepared [$^{13}C_2$]-L-**1** and [$^{13}C_5$]-L-**1** (Fig. S25†). The peak for ester carbonyl carbon at 169 ppm in the spectrum of the photoredox reaction mixture obtained using [$^{13}C_5$]-L-**1** at −20 °C suggested that **Co-1** probably inserted regioselectively

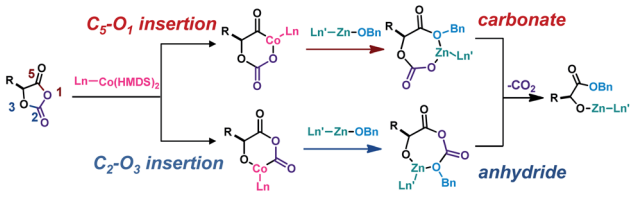

Scheme 6 Plausible oxidative insertion reactions between *O*-carboxyanhydrides and Co/Zn complexes.

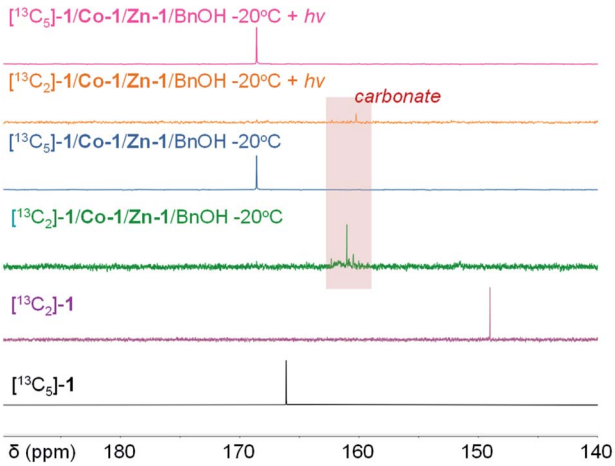

Fig. 3 ^{13}C NMR studies of oxidative addition reactions between L-**1** and Co/Zn complexes. To improve the ^{13}C NMR spectra qualities (due to the paramagnetic Co complexes) and determine the regioselectivity, [$^{13}C_2$]-**1** and [$^{13}C_5$]-**1** were used to study the ring-opening reaction (600 MHz, THF-d_8). The red area highlighted in spectra indicates $^{13}C_2$(O) carbonate peaks. [L-**1**]/[**Co-1**]/[**Zn-1**]/[BnOH] = 1/1/1/1.

into the O_1–C_5 bond of L-**1** (Fig. 3), in a manner similar to that observed for ROP of *N*-carboxyanhydrides[81] and our previously reported Ni/Zn/Ir-mediated photoredox ROP.[22,31] Only a small carbonate peak at 160 ppm was observed in the ^{13}C NMR spectra obtained when [$^{13}C_2$]-L-**1** was used in the photoredox reaction at −20 °C (Fig. 3, orange line), indicating that efficient photoredox decarboxylation occurred after the oxidative insertion. In contrast, in the absence of light at −20 °C, the same mixture showed multiple peaks at 163–160 ppm in the ^{13}C NMR spectrum (Fig. 3, green line), suggesting that decarboxylation was inefficient without light irradiation. Note that mixing **Co-1** with BnOH in the absence of L-**1** led to the formation of a precipitate, which rules out the possibility that a Co–alkoxide inserted into L-**1**.

Additionally, the ESI-MS spectrum obtained for the reaction mixture of L-**1**/**Co-1**/**Zn-1**/BnOH at room temperature rather than at −15 °C exhibited two sets of peaks, suggesting that side reactions occurred at room temperature (Fig. S26a†). We initially speculated that decarbonylation at room temperature occurred, similar to the case of Ni/Zn/Ir-mediated ROP of OCA. However, Fourier transform IR spectroscopy indicated no obvious Co–carbonyl peaks (~1940 cm^{-1}) were observed in the mixtures of L-**1**/**Co-1** (1/1) and L-**1**/**Co-1**/**Zn-1**/BnOH (1 equiv. of each), even in the presence of $(PPh_3)_3RhCl$, an extremely effective CO scavenger (Fig. S27†).[82] We thus hypothesized that the alkoxy radical species, which was generated following decarboxylation, could mediate a chain-scission side reaction at room temperature (Scheme 7). The alkoxy radical-mediated β-scission-like reaction has been recently reported in Ce and Mn mediated photoredox reactions.[53,83–85] It is also known that free primary alcohols are good *O*-nucleophiles and prone to 2e$^-$ oxidations that generate carboxylic acids or aldehydes under oxidative conditions.[52,53] We noticed that the absence of Zn complex seemed to not affect this side reaction (Fig. S26b†). This radical-mediated side reaction can be completely suppressed in the cold temperature (Fig. S26c†), which may explain the temperature's influence on the chain propagation and MWs shown in Fig. 1A.

On the basis of our results, we propose the following mechanism (Scheme 5). First, regioselective oxidative addition of Co^{II} complex to OCA leads to a transient Co^{III} intermediate **I**, which can be photoexcited to produce a strong photo-oxidant **II**. Next, the photoexcited cobaltacycle undergoes decarboxylation, which is thermodynamically feasible based on photophysical and electrochemical studies, to generate alkoxyl radical species **III** and reduced Co^{II} species. Although it remains unclear how a reactive alkoxy radical mediates chain-scission side reactions at room temperature,[86,87] at this point, we believe that this radical species should be rapidly intercepted by the Zn complex to generate a reactive Zn–alkoxide terminus at low temperature, thereby enabling the regeneration of the Co^{II} catalyst.

Discovery of Co/Hf-mediated photoredox polymerization of OCAs

Based on our success of using Co/Zn complexes for photoredox ROP of OCAs, it was conceivable that other metal alkoxides may replace Zn–alkoxides to promote chain propagation in the polymerization. We then began our investigation by screening the reactivity of different metal alkoxides, *e.g.*, Zr, Hf, Y, and *in situ* prepared Mg–alkoxides in the photoredox polymerization of L-**1** in the presence of Co complexes at −15 °C (Table S7†). We found that the use of **Co-2** (Scheme 8), a Co^{II} complex with a less bulky pyridine ligand than that of **Co-1**, together with hafnium isopropoxide showed decent polymerization activities (entry 2 *versus* 1), yet with little control over the MWs when adjusting the monomer to catalyst feeding ratios (entries 2–4). Notably, the substitute of **Co-2** with (bpy)Ni/**Ir-1** resulted in the diminished reactivity (entry 5); and hafnium isopropoxide itself was unable to initiate polymerization (entry 6). Other metal alkoxides (Zr, Y

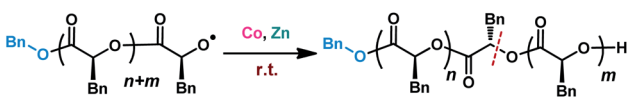

Scheme 7 Plausible radical-induced chain scission side reactions at room temperature.

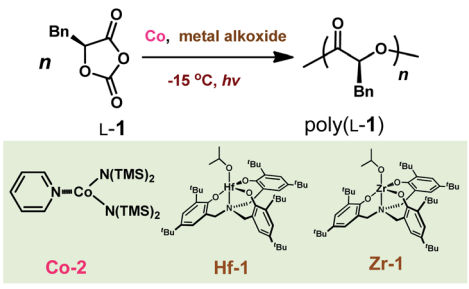

Scheme 8 Co/Hf- or Co/Zn-mediated photoredox ring-opening polymerization.

and Mg) were essentially unreactive towards L-**1** (entries 7–9). The addition of macrodentate complex to Hf alkoxide that forms **Hf-1** (Scheme 8) enhanced the reactivity with an increased M_n value of 91.0 kDa, and a narrow $Đ$ of 1.02 (entries 10–11). However, such strategy did not work for Zr complexes (entry 12). Our results agree with the recent studies about the reactivities of metal alkoxides or silylamides towards ROP of OCAs by other groups,[88,89] which may be related to the decarboxylation capability of metal complexes.[90] To this end, the identification of the active Hf complexes allows us to carry out stereoselective photoredox ROPs to synthesize different stereoregular polymers (*vide infra*).

Stereoselective photoredox ring-opening polymerization of OCAs

We next explored whether our methods could be applied to stereoselective photoredox ROP of racemic OCAs. Similar to our studies in eROP, we found that the ligand of the Co complex markedly affected the polymerization stereoselectivity: under the optimized photoredox conditions at −15 °C, the use of **Zn-2** and **Co-1** ([L-**1**]/[D-**1**]/[**Co-1**]/[**Zn-2**]/[BnOH] = 150/150/1/1/1; Scheme 9) afforded a stereoblock (*sb*) copolymer poly(*sb*-**1**) with a M_n of 67.0 kDa, a narrow $Đ$ of 1.05, and a high P_m of 0.96 (P_m, probability of meso dyad formation; Table S8, entry 1; Fig. S30a†). In contrast, **Co-2**/**Zn-3** initiated controlled polymerization of *rac*-**1** ([L-**1**]/[D-**1**]/[**Co-2**]/[**Zn-3**]/[BnOH] = 100/100/1/1/1) and afforded syndiotactic (*sd*) copolymer poly(*sd*-**1**) with a P_r (probability of racemic dyad formation) of 0.88 (M_n = 57.7 kDa, $Đ$ = 1.14; entry 2; Fig. S30b†). Note that when **Zn-2** was replaced with **Zn-1**, polymerization was not efficiently initiated (entries 3–4); when **Co-2** was replaced by **Co-1**, the obtained polymer had a large $Đ$ of 1.28 and a decreased P_r value (entry 5; Fig. S30c†); **Zn-2** or **Zn-3** alone was incapable to initiate polymerization of *rac*-**1** (entries 6–7). Either the increase of steric bulky group or introducing electron-withdrawing cyano substituent on the β-diimine ligand of **Zn-3** could not improve the syndioselectivity of the polymerization (entries 8–9; Fig. S30d and e†).

Additionally, we found that the combination of **Co-2** with **Hf-1** (Scheme 9), a reported syndioselective Hf–alkoxide complex for *rac*-lactide and *rac*-**4** polymerization,[88,91] provided syndiotactic copolymers when used for the photoredox ROP of *rac*-**1** with a P_r of 0.89 ([L-**1**]/[D-**1**]/[**Co-2**]/[**Hf-1**] = 200/200/1/1; M_n = 96.6 kDa, $Đ$ = 1.06; Table S8, entry 10; Fig. S30f†). Changing the [L-**1**]/[D-**1**] ratio from 1/1 to 2/1 or 1/2 markedly decreased the P_r value from 0.89 to 0.77 ([**Co-2**]/[**Hf-1**] = 1/1, entries 12–13 *versus* 11), confirming our assigned tetrad peaks. Kinetic studies agreed well with our measured syndioselectivity that $k_{RS} \gg k_{RR} \sim k_{SS}$ in both **Co-2**/**Zn-3** and **Co-2**/**Hf-1** catalytic systems (Fig. S31a and b†). The use of **Hf-2** with less sterically bulky ligand compared to **Hf-1** did not improve the P_r value (entry 15; Fig. S30g†); whereas the sole use of Hf complexes was found to be essentially unreactive towards *rac*-**1** (entries 16–17), different from the literature.[88]

We next demonstrated that such stereoselective photoredox ROPs could be extended to other OCA monomers (Scheme 10). Notably, the stereoselectivity trends that were observed in ROP of *rac*-**1** varied in other monomers. For example, **Co-1**/**Zn-2** and **Co-2**/**Zn-3** exhibited similar isoselectivity in the photoredox ROPs of *rac*-**2** and *rac*-**4** (Scheme 10A; Table S9, entries 1–2 and 4–5; Fig. S32 and S33†). Intriguingly, the photoredox ROP of *rac*-**4** using **Co-2**/**Hf-1** resulted in stereoblock copolymers, with a P_m of 0.74 ([L-**4**]/[D-**4**]/[**Co-2**]/[**Hf-1**] = 200/200/1/1; M_n = 32.8 kDa, $Đ$ = 1.04; entry 6; Fig. S33c†), contrast to a syndiotactic poly(*sd*-**4**) generated by **Hf-1** alone (P_r = 0.82; entry 7; Fig. S33d†). Kinetic studies are consistent with the formation of a stereoblock copolymer: the copolymerization of *rac*-**4** was much slower than the polymerization of either enantiomer separately at the same [**4**]/[**Hf-1**] ratio under the same conditions (Fig. S31c†), which excludes the possibility that two isotactic polymers, poly(L-**4**) and poly(D-**4**), formed separately.

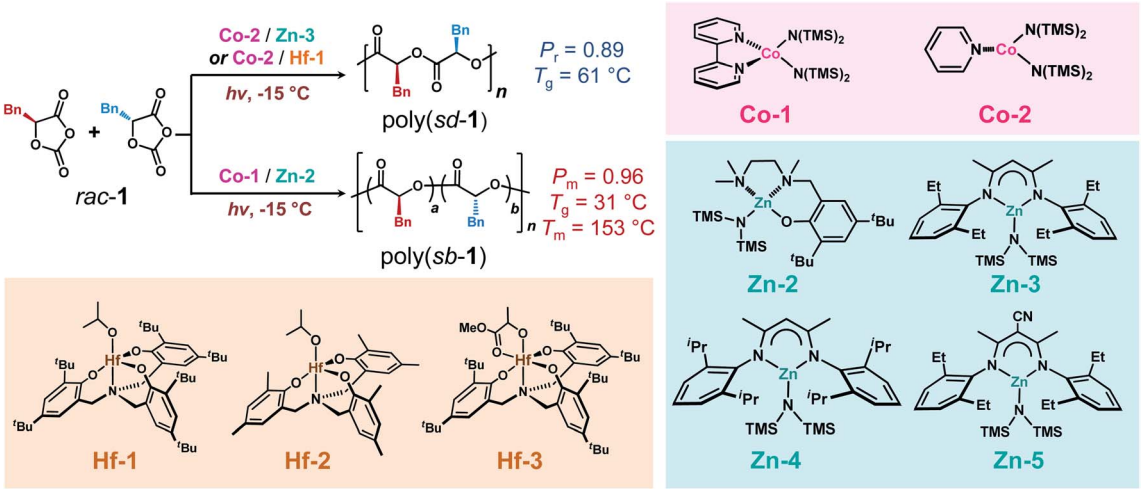

Scheme 9 Stereoselective photoredox ring-opening polymerization of racemic monomer **1** mediated by Co/Zn and Co/Hf complexes to prepare polymers with stereoblock or syndiotactic microstructures.[a] [a]Abbreviations: P_m, maximum probability of meso dyad formation; P_r, maximum probability of racemic dyad formation; T_g, glass transition temperature; T_m, melting temperature; *sb*, stereoblock; *sd*, syndiotactic. See Table S8† for detailed polymerization data.

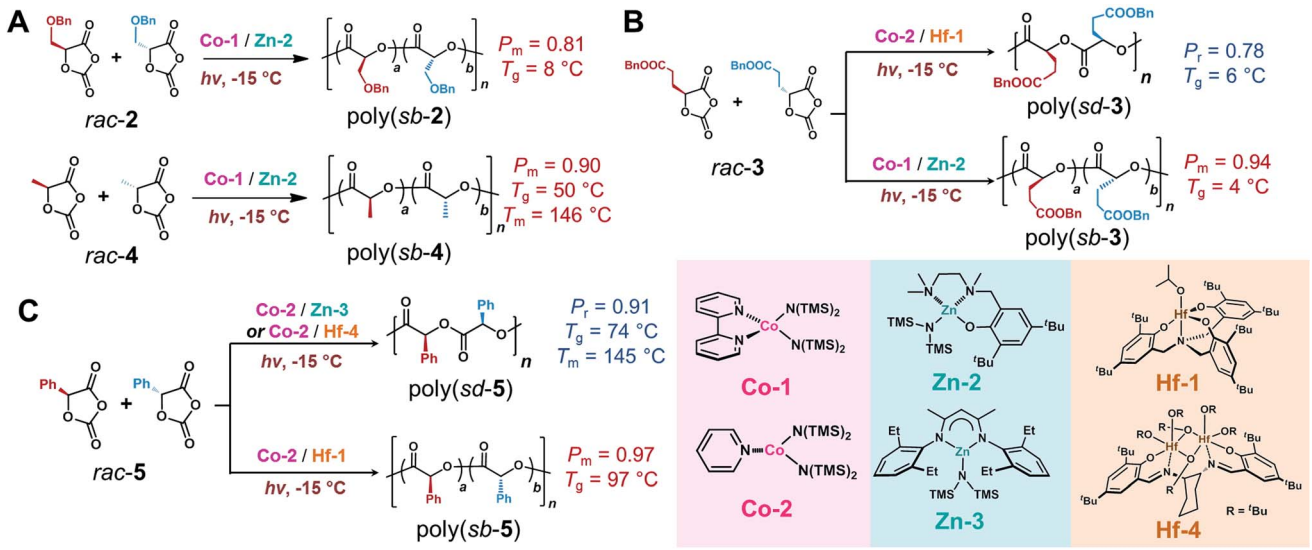

Scheme 10 Stereoselective photoredox ring-opening polymerization of racemic *O*-carboxyanhydrides (A) **2** and **4**, (B) **3**, and (C) **5**, which are mediated by Co/Zn and Co/Hf complexes.[a] [a]Abbreviations: P_m, maximum probability of meso dyad formation; P_r, maximum probability of racemic dyad formation; T_g, glass transition temperature; T_m, melting temperature; *sb*, stereoblock; *sd*, syndiotactic. See Table S9† for detailed polymerization data.

On the other hand, **Co-1**/**Zn-2** provided stereoblock copolymers in the photoredox ROPs of *rac*-**3** and *rac*-**5** (Scheme 10B and C; Table S9,† entries 8 and 11), with P_m values of 0.94 and 0.77, respectively (Fig. S34a and S35a†); whereas **Co-2**/**Zn-3** exhibited moderate syndioselectivity (entries 9 and 12; Fig. S34b and S35b†). However, **Co-2**/**Hf-1** showed syndioselectivity towards *rac*-**3** (entry 10; Fig. S34c†), but could mediate isoselective synthesis of poly(*sb*-**5**) with a P_m of 0.97 (entry 13; Fig. S35c†). Furthermore, in the presence of **Co-2**, the replacement of **Hf-1** with **Hf-4** (Scheme 10), a dinuclear hafnium complex, resulted in the syndioselective photoredox ROP of *rac*-**5** with a P_r of 0.91 (entry 14; Fig. S35d†). Importantly, we found that T_g values increase as the syndiotacticity P_r values increase in poly(*rac*-**1**), higher than their stereoblock and isotactic counterparts (Table S10, entries 1–3; Fig. S36†), similar to the cases in poly(methyl methacrylate)[92] and poly(3-hydroxybutyrate).[93,94] However, such trend is reserved in the case of poly(**5**): obtained poly(*sb*-**5**) had a T_g of 97 °C, which was similar to that of poly(L-**5**) and much higher than that of poly(*sd*-**5**) (74 °C; Fig. S40;† entries 11–15), similar to that observed in poly(lactide).[24,95] Our photoredox ROP thus offers stereoregular polymers with T_g values spanning over ~100 °C (poly(*sb*-**3**) to poly(*sb*-**5**), Table S10†). Notably, stereocomplex (*sc*) of polyesters[96] can also lead to polymers exhibiting melting temperatures that are not found in other microstructures (*e.g.*, poly(*sc*-**5**), entry 16). To be practically useful in many applications, polymers are expected to have thermal transitions far from room temperature. Specifically, polyesters with T_g values above approximately 90 °C are useful for applications in which a rigid structure must be maintained, such as preventing polyesters deformation in the presence of hot water. The wide range of T_g values also potentially allows for the preparation of multiblock thermoplastic elastomers.[97–99]

Conclusions

Our work represents an important proof of concept that a catalytic system can mediate controlled ROP by either light (this report) or electricity.[32] We have demonstrated that the oxidation status of Co complexes can be modulated by application of light during the polymerization, without the assistance from rare transition metal photocatalysts such as Ru or Ir complexes. Given the growing interest in replacing polyolefins with degradable and recyclable polymers,[1] the discovery of Co/Zn catalytic system provides an alternative paradigm to develop stimulus-triggered polymerization strategies in coordination polymerization chemistry.

Synergism between metal catalysts has been recently used to improve ROP performances, including using hetrodinuclear catalysts for the ROP of LA,[100] and the copolymerization of CO_2 and epoxides.[101,102] In the case of photoredox ROP of OCAs, combining two metal catalysts not only significantly enhances the reactivity to produce high-MW PAHAs, but also allows for precise control of polymer's tacticity, which can significantly affect PAHA's thermal properties. To our knowledge, most photo- and electrochemically controlled polymerization strategies in polyolefins, however, could not mediate stereoselective polymerization.

Collectively, we believe that this stimulus-triggered controlled polymerization chemistry will prove to be widely applicable in polymer and materials research. Ongoing studies are directed toward the synthesis of new metal initiators to regulate stereoselectivity as well as functionalized polyesters for future production of tough polyesters and thermoplastic elastomers.

Author contributions

Y. Z., Q. F., and R. T. conceived the idea and designed experiments. Y. Z., Q. F., X. W. performed experiments. L. Y.

performed density functional theory calculations. A. G. K. performed diffusion-ordered NMR spectroscopy experiments. Y. Z., Q. F., X. W. L. A. M., and R. T. analyzed the data. Y. Z. and R. T. wrote the manuscript.

Conflicts of interest

Provisional patents (U.S. Patent Application No: 62/414016 and VTIP No. 19-112) have been filed pertaining to the results presented in this paper. The authors declare no other competing interests.

Acknowledgements

This work was supported by start-up funding from Virginia Tech, ACS-Petroleum Research Foundation (57926-DNI-7), and the National Science Foundation (CHE-1807911). We thank Dr N. Murthy Shanaiah for NMR experiments, Mehdi Ashraf-Khorassani for electrospray ionization mass spectrometry studies, Dr Jeffrey Parks for inductively coupled plasma mass spectrometry measurements, Dr Amanda Morris for fluorescence spectra measurements, Dr Guoliang Liu for differential scanning calorimetry, and Dr Webster Santos and Dr John Matson (all from Virginia Tech, Department of Chemistry) for providing anhydrous solvents.

References

1 Y. Zhu, C. Romain and C. K. Williams, *Nature*, 2016, **540**, 354–362.
2 K. Sudesh, H. Abe and Y. Doi, *Prog. Polym. Sci.*, 2000, **25**, 1503–1555.
3 M. A. Hillmyer and W. B. Tolman, *Acc. Chem. Res.*, 2014, **47**, 2390–2396.
4 J.-B. Zhu, E. M. Watson, J. Tang and E. Y.-X. Chen, *Science*, 2018, **360**, 398–403.
5 T. Hayashi, *Prog. Polym. Sci.*, 1994, **19**, 663–702.
6 B. Martin Vaca and D. Bourissou, *ACS Macro Lett.*, 2015, **4**, 792–798.
7 Q. Yin, L. Yin, H. Wang and J. Cheng, *Acc. Chem. Res.*, 2015, **48**, 1777–1787.
8 R. Tong, *Ind. Eng. Chem. Res.*, 2017, **56**, 4207–4219.
9 M. Yin and G. L. Baker, *Macromolecules*, 1999, **32**, 7711–7718.
10 F. Jing, M. R. Smith and G. L. Baker, *Macromolecules*, 2007, **40**, 9304–9312.
11 G. L. Baker, E. B. Vogel and M. R. Smith, *Polym. Rev.*, 2008, **48**, 64–84.
12 T. L. Simmons and G. L. Baker, *Biomacromolecules*, 2001, **2**, 658–663.
13 Y. Yu, J. Zou and C. Cheng, *Polym. Chem.*, 2014, **5**, 5854–5872.
14 R. T. Martin, L. P. Camargo and S. A. Miller, *Green Chem.*, 2014, **16**, 1768–1773.
15 S. A. Cairns, A. Schultheiss and M. P. Shaver, *Polym. Chem.*, 2017, **8**, 2990–2996.
16 Y. Xu, M. R. Perry, S. A. Cairns and M. P. Shaver, *Polym. Chem.*, 2019, **10**, 3048–3054.
17 O. T. du Boullay, E. Marchal, B. Martin-Vaca, F. P. Cossio and D. Bourissou, *J. Am. Chem. Soc.*, 2006, **128**, 16442–16443.
18 Y. Zhong and R. Tong, *Front. Chem.*, 2018, **6**, 641.
19 R. J. Pounder, D. J. Fox, I. A. Barker, M. J. Bennison and A. P. Dove, *Polym. Chem.*, 2011, **2**, 2204–2212.
20 A. Buchard, D. R. Carbery, M. G. Davidson, P. K. Ivanova, B. J. Jeffery, G. I. Kociok-Köhn and J. P. Lowe, *Angew. Chem., Int. Ed.*, 2014, **53**, 13858–13861.
21 R. Wang, J. Zhang, Q. Yin, Y. Xu, J. Cheng and R. Tong, *Angew. Chem., Int. Ed.*, 2016, **55**, 13010–13014.
22 Q. Feng and R. Tong, *J. Am. Chem. Soc.*, 2017, **139**, 6177–6182.
23 Q. Feng, Y. Zhong, L. Xie and R. Tong, *Synlett*, 2017, **28**, 1857–1866.
24 M. J. Stanford and A. P. Dove, *Chem. Soc. Rev.*, 2010, **39**, 486–494.
25 J.-F. Lutz, D. Neugebauer and K. Matyjaszewski, *J. Am. Chem. Soc.*, 2003, **125**, 6986–6993.
26 B. M. Chamberlain, M. Cheng, D. R. Moore, T. M. Ovitt, E. B. Lobkovsky and G. W. Coates, *J. Am. Chem. Soc.*, 2001, **123**, 3229–3238.
27 O. Dechy-Cabaret, B. Martin-Vaca and D. Bourissou, *Chem. Rev.*, 2004, **104**, 6147–6176.
28 N. Ajellal, J.-F. Carpentier, C. Guillaume, S. M. Guillaume, M. Helou, V. Poirier, Y. Sarazin and A. Trifonov, *Dalton Trans.*, 2010, **39**, 8363–8376.
29 C. M. Thomas, *Chem. Soc. Rev.*, 2010, **39**, 165–173.
30 S. M. Guillaume, E. Kirillov, Y. Sarazin and J.-F. Carpentier, *Chem.–Eur. J.*, 2015, **21**, 7988–8003.
31 Q. Feng, L. Yang, Y. Zhong, D. Guo, G. Liu, L. Xie, W. Huang and R. Tong, *Nat. Commun.*, 2018, **9**, 1559.
32 Y. Zhong, Q. Feng, X. Wang, J. Chen, W. Cai and R. Tong, *ACS Macro Lett.*, 2020, **9**, 1114–1118.
33 N. A. Romero and D. A. Nicewicz, *Chem. Rev.*, 2016, **116**, 10075–10166.
34 B. J. Shields, B. Kudisch, G. D. Scholes and A. G. Doyle, *J. Am. Chem. Soc.*, 2018, **140**, 3035–3039.
35 C. B. Larsen and O. S. Wenger, *Chem.–Eur. J.*, 2018, **24**, 2039–2058.
36 O. Reiser, *Acc. Chem. Res.*, 2016, **49**, 1990–1996.
37 A. Hossain, A. Bhattacharyya and O. Reiser, *Science*, 2019, **364**, eaav9713.
38 Q. M. Kainz, C. D. Matier, A. Bartoszewicz, S. L. Zultanski, J. C. Peters and G. C. Fu, *Science*, 2016, **351**, 681–684.
39 D. M. Flores and V. A. Schmidt, *J. Am. Chem. Soc.*, 2019, **141**, 8741–8745.
40 M. E. Weiss, L. M. Kreis, A. Lauber and E. M. Carreira, *Angew. Chem., Int. Ed.*, 2011, **50**, 11125–11128.
41 B. D. Ravetz, J. Y. Wang, K. E. Ruhl and T. Rovis, *ACS Catal.*, 2019, **9**, 200–204.
42 E. Bergamaschi, F. Beltran and C. J. Teskey, *Chem.–Eur. J.*, 2020, **26**, 5180–5184.

43 W.-Q. Liu, T. Lei, S. Zhou, X.-L. Yang, J. Li, B. Chen, J. Sivaguru, C.-H. Tung and L.-Z. Wu, *J. Am. Chem. Soc.*, 2019, **141**, 13941–13947.
44 C.-H. Lim, M. Kudisch, B. Liu and G. M. Miyake, *J. Am. Chem. Soc.*, 2018, **140**, 7667–7673.
45 X. Shen, Y. Li, Z. Wen, S. Cao, X. Hou and L. Gong, *Chem. Sci.*, 2018, **9**, 4562–4568.
46 Y. Gao, C. Yang, S. Bai, X. Liu, Q. Wu, J. Wang, C. Jiang and X. Qi, *Chem*, 2020, **6**, 675–688.
47 P. Nuhant, M. S. Oderinde, J. Genovino, A. Juneau, Y. Gagné, C. Allais, G. M. Chinigo, C. Choi, N. W. Sach, L. Bernier, Y. M. Fobian, M. W. Bundesmann, B. Khunte, M. Frenette and O. O. Fadeyi, *Angew. Chem., Int. Ed.*, 2017, **56**, 15309–15313.
48 L. Wang, J. M. Lear, S. M. Rafferty, S. C. Fosu and D. A. Nagib, *Science*, 2018, **362**, 225.
49 R.-Z. Liu, J. Li, J. Sun, X.-G. Liu, S. Qu, P. Li and B. Zhang, *Angew. Chem., Int. Ed.*, 2020, **59**, 4428–4433.
50 Y. Qiao, Q. Yang and E. J. Schelter, *Angew. Chem., Int. Ed.*, 2018, **57**, 10999–11003.
51 A. Hu, J.-J. Guo, H. Pan and Z. Zuo, *Science*, 2018, **361**, 668–672.
52 K. Zhang, L. Chang, Q. An, X. Wang and Z. Zuo, *J. Am. Chem. Soc.*, 2019, **141**, 10556–10564.
53 Q. An, Z. Wang, Y. Chen, X. Wang, K. Zhang, H. Pan, W. Liu and Z. Zuo, *J. Am. Chem. Soc.*, 2020, **142**, 6216–6226.
54 J.-H. Ye, M. Miao, H. Huang, S.-S. Yan, Z.-B. Yin, W.-J. Zhou and D.-G. Yu, *Angew. Chem., Int. Ed.*, 2017, **56**, 15416–15420.
55 X.-J. Wei, I. Abdiaj, C. Sambiagio, C. Li, E. Zysman-Colman, J. Alcázar and T. Noël, *Angew. Chem., Int. Ed.*, 2019, **58**, 13030–13034.
56 W.-M. Cheng and R. Shang, *ACS Catal.*, 2020, **10**, 9170–9196.
57 F. Glaser and O. S. Wenger, *Coord. Chem. Rev.*, 2020, **405**, 213129.
58 M. C. Carey, S. L. Adelman and J. K. McCusker, *Chem. Sci.*, 2019, **10**, 134–144.
59 J. K. McCusker, *Science*, 2019, **363**, 484–488.
60 C. Theunissen, M. A. Ashley and T. Rovis, *J. Am. Chem. Soc.*, 2019, **141**, 6791–6796.
61 M. Li, Y. Tao, J. Tang, Y. Wang, X. Zhang, Y. Tao and X. Wang, *J. Am. Chem. Soc.*, 2019, **141**, 281–289.
62 C. K. Prier, D. A. Rankic and D. W. C. MacMillan, *Chem. Rev.*, 2013, **113**, 5322–5363.
63 D. M. Schultz and T. P. Yoon, *Science*, 2014, **343**, 1239176.
64 J. W. Tucker and C. R. J. Stephenson, *J. Org. Chem.*, 2012, **77**, 1617–1622.
65 M. Chen, M. Zhong and J. A. Johnson, *Chem. Rev.*, 2016, **116**, 10167–10211.
66 J. C. Theriot, C.-H. Lim, H. Yang, M. D. Ryan, C. B. Musgrave and G. M. Miyake, *Science*, 2016, **352**, 1082–1086.
67 S. Dadashi-Silab, S. Doran and Y. Yagci, *Chem. Rev.*, 2016, **116**, 10212–10275.
68 N. Corrigan, S. Shanmugam, J. Xu and C. Boyer, *Chem. Soc. Rev.*, 2016, **45**, 6165–6212.
69 T. G. Ribelli, D. Konkolewicz, S. Bernhard and K. Matyjaszewski, *J. Am. Chem. Soc.*, 2014, **136**, 13303–13312.
70 D. Konkolewicz, K. Schröder, J. Buback, S. Bernhard and K. Matyjaszewski, *ACS Macro Lett.*, 2012, **1**, 1219–1223.
71 M. S. Lowry, J. I. Goldsmith, J. D. Slinker, R. Rohl, R. A. Pascal, G. G. Malliaras and S. Bernhard, *Chem. Mater.*, 2005, **17**, 5712–5719.
72 M. Haga, E. S. Dodsworth, G. Eryavec, P. Seymour and A. B. P. Lever, *Inorg. Chem.*, 1985, **24**, 1901–1906.
73 A. C. Albéniz, P. Espinet, R. López-Fernández and A. Sen, *J. Am. Chem. Soc.*, 2002, **124**, 11278–11279.
74 J. R. Carney, B. R. Dillon, L. Campbell and S. P. Thomas, *Angew. Chem., Int. Ed.*, 2018, **57**, 10620–10624.
75 G. Auböck and M. Chergui, *Nat. Chem.*, 2015, **7**, 629–633.
76 D. M. Arias-Rotondo and J. K. McCusker, *Chem. Soc. Rev.*, 2016, **45**, 5803–5820.
77 Z. W. Zuo, D. T. Ahneman, L. L. Chu, J. A. Terrett, A. G. Doyle and D. W. C. MacMillan, *Science*, 2014, **345**, 437–440.
78 Z. Zuo and D. W. C. MacMillan, *J. Am. Chem. Soc.*, 2014, **136**, 5257–5260.
79 P. P. Power, *Chem. Rev.*, 2012, **112**, 3482–3507.
80 W. Bermel, I. Bertini, I. C. Felli, R. Kümmerle and R. Pierattelli, *J. Am. Chem. Soc.*, 2003, **125**, 16423–16429.
81 T. J. Deming and S. A. Curtin, *J. Am. Chem. Soc.*, 2000, **122**, 5710–5717.
82 K. R. Dunbar and S. C. Haefner, *Inorg. Chem.*, 1992, **31**, 3676–3679.
83 J.-J. Guo, A. Hu and Z. Zuo, *Tetrahedron Lett.*, 2018, **59**, 2103–2111.
84 B. D. W. Allen, M. D. Hareram, A. C. Seastram, T. McBride, T. Wirth, D. L. Browne and L. C. Morrill, *Org. Lett.*, 2019, **21**, 9241–9246.
85 J. Zhang, Y. Li, F. Zhang, C. Hu and Y. Chen, *Angew. Chem., Int. Ed.*, 2016, **55**, 1872–1875.
86 A. Padwa, *J. Org. Chem.*, 2009, **74**, 6421–6441.
87 L. Capaldo and D. Ravelli, *Chem. Commun.*, 2019, **55**, 3029–3032.
88 Y. Sun, Z. Jia, C. Chen, Y. Cong, X. Mao and J. Wu, *J. Am. Chem. Soc.*, 2017, **139**, 10723–10732.
89 Y. Wang and T.-Q. Xu, *Macromolecules*, 2020, **53**, 8829–8836.
90 D. H. Gibson, *Chem. Rev.*, 1996, **96**, 2063–2096.
91 A. J. Chmura, M. G. Davidson, C. J. Frankis, M. D. Jones and M. D. Lunn, *Chem. Commun.*, 2008, **47**, 1293–1295.
92 L. R. Denny, R. F. Boyer and H.-G. Ellas, *J. Macromol. Sci., Part B: Phys.*, 1986, **25**, 227–265.
93 N. Ajellal, M. Bouyahyi, A. Amgoune, C. M. Thomas, A. Bondon, I. Pillin, Y. Grohens and J.-F. Carpentier, *Macromolecules*, 2009, **42**, 987–993.
94 X. Tang and E. Y. X. Chen, *Nat. Commun.*, 2018, **9**, 2345.
95 T. M. Ovitt and G. W. Coates, *J. Am. Chem. Soc.*, 2002, **124**, 1316–1326.
96 H. Tsuji, *Macromol. Biosci.*, 2005, **5**, 569–597.
97 F. S. Bates, M. A. Hillmyer, T. P. Lodge, C. M. Bates, K. T. Delaney and G. H. Fredrickson, *Science*, 2012, **336**, 434–440.

98 G. L. Gregory, G. S. Sulley, L. P. Carrodeguas, T. T. D. Chen, A. Santmarti, N. J. Terrill, K.-Y. Lee and C. K. Williams, *Chem. Sci.*, 2020, **11**, 6567–6581.
99 G. S. Sulley, G. L. Gregory, T. T. D. Chen, L. Peña Carrodeguas, G. Trott, A. Santmarti, K.-Y. Lee, N. J. Terrill and C. K. Williams, *J. Am. Chem. Soc.*, 2020, **142**, 4367–4378.
100 A. B. Kremer and P. Mehrkhodavandi, *Coord. Chem. Rev.*, 2019, **380**, 35–57.
101 J. A. Garden, P. K. Saini and C. K. Williams, *J. Am. Chem. Soc.*, 2015, **137**, 15078–15081.
102 A. C. Deacy, A. F. R. Kilpatrick, A. Regoutz and C. K. Williams, *Nat. Chem.*, 2020, **12**, 372–380.